SOURCE DATA · TRANSPARENT PROCESS · OPEN ACCESS

A microRNA cluster in the Fragile-X region expressed during spermatogenesis targets FMR1

Madhuvanthi Ramaiah[1],[†], Kun Tan[1],[†] iD, Terra-Dawn M Plank[1], Hye-Won Song[1], Jennifer N Dumdie[1], Samantha Jones[1], Eleen Y Shum[1], Steven D Sheridan[2],[3], Kevin J Peterson[4], Jörg Gromoll[5], Stephen J Haggarty[2],[3], Heidi Cook-Andersen[1],[6] & Miles F Wilkinson[1],[7],[*] iD

Abstract

Testis-expressed X-linked genes typically evolve rapidly. Here, we report on a testis-expressed X-linked microRNA (miRNA) cluster that despite rapid alterations in sequence has retained its position in the Fragile-X region of the X chromosome in placental mammals. Surprisingly, the miRNAs encoded by this cluster (*Fx-mir*) have a predilection for targeting the immediately adjacent gene, *Fmr1*, an unexpected finding given that miRNAs usually act *in trans*, not *in cis*. Robust repression of *Fmr1* is conferred by combinations of *Fx-mir* miRNAs induced in Sertoli cells (SCs) during postnatal development when they terminate proliferation. Physiological significance is suggested by the finding that FMRP, the protein product of *Fmr1*, is downregulated when *Fx-mir* miRNAs are induced, and that FMRP loss causes SC hyperproliferation and spermatogenic defects. *Fx-mir* miRNAs not only regulate the expression of FMRP, but also regulate the expression of eIF4E and CYFIP1, which together with FMRP form a translational regulatory complex. Our results support a model in which *Fx-mir* family members act cooperatively to regulate the translation of batteries of mRNAs in a developmentally regulated manner in SCs.

Introduction

Conventional wisdom holds that conserved genes are critical for biological processes. However, an emerging area of interest is rapidly diverging genes, as these have the potential to confer species-specific traits while simultaneously retaining ancient functions [1,2]. Testes-expressed genes are a particularly rich source of genes undergoing rapid evolution [3,4]. While the underlying mechanism is not known, evidence suggests that strong selection pressures—including post-copulatory sexual selection mechanisms (e.g., sperm competition)—drive the rapid sequence alterations in testes-expressed genes [5–9]. Particularly enriched for rapidly evolving genes is the mammalian X chromosome, in part, because it is single copy in males and thus can allow for rapid fixation of sequence alterations that confer a selective advantage in spermatogenesis and other male-associated functions [10–14].

In this communication, we investigate the evolution, expression, and function of an X-linked microRNA (miRNA) cluster. miRNAs are small (~22 nt) RNAs that regulate gene expression through translational repression or destabilization of their target transcripts [15–17]. Mammalian genomes encode hundreds of miRNAs, many of which are spatially and temporally regulated [18]. In turn, each miRNA can potentially target hundreds of mRNAs [19]. miRNAs have important functions in many aspects of cellular differentiation and homeostasis, and consequently have roles in many pathologies, including cancer, neural disease, and infertility [20–22]. About 40% of microRNAs are estimated to form clusters whose physiological importance is largely unknown [23]. In contrast, the roles of individual miRNAs have been defined in a variety of physiological and pathological states [24,25].

In this report, we report the discovery of a miRNA cluster in the Fragile-X region of the X chromosome with unusual functional qualities that has undergone rapid evolution in placental mammals. The miRNAs encoded by this cluster are primarily expressed in the testis, thereby providing an explanation for their rapid evolution. Given that miRNAs act *in trans*, not *in cis*, we were surprised to find that a large number of the miRNAs in this Fragile-X cluster target the immediately adjacent gene: *FMR1*. Indeed, the position of this

1 Department of Obstetrics, Gynecology, and Reproductive Sciences, University of California, San Diego, La Jolla, CA, USA
2 Chemical Neurobiology Laboratory, Center for Genomic Medicine, Boston, MA, USA
3 Departments of Neurology and Psychiatry, Massachusetts General Hospital, Boston, MA, USA
4 Department of Biological Sciences, Dartmouth College, Hanover, NH, USA
5 Center for Reproductive Medicine and Andrology, University of Münster, Münster, Germany
6 Division of Biological Sciences, University of California, San Diego, La Jolla, CA, USA
7 Institute of Genomic Medicine, University of California, San Diego, La Jolla, CA, USA
*Corresponding author. Tel: +1 858 8224819; Fax: +1 858 5348329; E-mail: mfwilkinson@ucsd.edu
†These authors contributed equally to this work

miRNA cluster next to *FMR1* is evolutionarily conserved in placental mammals. Given that *FMR1* encodes a translational regulator [26], we examined the role of members of this Fragile-X miRNA cluster in regulating translation, as well as the biological contexts in which it acts. Our findings have implications for evolution, spermatogenesis, and the diagnosis and treatment of male infertility.

Results

Fx-mir—a rapidly evolving miRNA cluster directly adjacent to *Fmr1*

Our long-term interest in miRNAs, X-linked gene clusters, and intellectual disability [27–31] led us to note the existence of a large group of miRNAs in the Fragile-X region of the mouse X chromosome (Fig 1A). The Fragile-X region is best known for housing the *FMR1* gene, which when mutated, causes Fragile-X Syndrome (FXS), the most common form of inherited intellectual disability in humans [32–34]. The Fragile-X region also harbors several other protein-coding genes that have been given the "Fragile X" designation (Appendix Fig S1A). Thus, we elected to name the miRNA cluster in this region the "Fragile-X miRNA (*Fx-mir*)" cluster. There are no annotated protein-coding genes interrupting the miRNA genes in the mouse *Fx-mir* cluster. All 22 miRNAs in this cluster are oriented in the same direction, raising the possibility that these miRNAs could all be derived from a single transcription unit.

To gain insight into the evolutionary origins of this cluster, we mapped the *Fx-mir* cluster in multiple species, based on available Ensembl assemblies. We examined three placental mammals [human (*Homo sapien*), dog (*Canis familiaris*), and elephant (*Loxodonta africana*)] in addition to mice and observed that all four of these mammalian species have a miRNA cluster between the *Fmr1* and *Slitrk2* protein-coding genes (Fig EV1). In contrast, no observable miRNA cluster is present in the non-placental mammal opossum (*Monodelphis domestica*) (Fig EV1). Although the *Slitrk2* gene appears to be specific to placental mammals, a broader syntenic analysis shows that the linear relationship between *Fmr1* and two upstream markers, *Fam122b* and the *miR-18b* miRNA cluster, is retained in all five species we examined, including opossum, thereby allowing us to unambiguously conclude that opossum lacks the *Fx-mir* cluster, at least at its chromosomal location in placental mammals. Together, our results indicate that the *Fx-mir* cluster is present at a conserved location in the Fragile-X region of placental mammals.

Because the human and mouse genomes are well annotated, we focused our subsequent analysis on the *Fx-mir* cluster in these two species. Both the mouse *Fx-mir* and human *FX-MIR* clusters consist of the same number of miRNAs (Figs 1A and B). Furthermore, all the miRNA genes are oriented in the same transcriptional direction in both the mouse and human clusters. In striking contrast to these conserved features, only one miRNA encoded by these clusters has retained sufficient sequence similarity in mice and humans to be clearly defined as an ortholog (Fig 1). This miRNA, *miR-509*, displayed considerable sequence identity between both mouse and humans throughout the length of its precursor (Appendix Fig S1B).

Furthermore, most of the seed sequence in mature *miR-509* is identical between mice and humans. To screen for other candidate orthologous miRNAs within this cluster, we aligned each of the 22 mouse *Fx-mir* miRNA precursor sequence with each of the 22 human *FX-MIR* precursor sequences (data not shown). This analysis revealed considerable sequence identity between the precursor sequences of mouse *miR-881* and human *miR-892a*, as well as between mouse *miR-880* and both human *miR-888* and miR-890 (Appendix Fig S1C). However, there is only limited sequence identity in the seed region, precluding defining these miRNAs as being definitive orthologs.

Mouse *Fx-mir* cluster family members target *Fmr1*

Using several miRNA target prediction programs, we noted that a frequent putative direct target of several members of the mouse *Fx-mir* cluster is *Fmr1*, the directly adjacent gene (Fig 1A). To systematically test the possibility that *Fx-mir* family members have a predilection for targeting *Fmr1*, we first performed an *in silico* screen to identify all miRNAs predicted to regulate *Fmr1*. We used two target prediction programs—TargetScan and microRNA.org—to increase the probability of identifying *bona fide* targets. Both conserved and non-conserved miRNAs were considered using the miRanda target sites and mirSVR scores provided by microRNA.org [35]. Appendix Table S1 lists the 15 miRNAs with the highest prediction scores of the 1,915 candidate mouse miRNAs in miRBase that were analyzed. Two of the top 15 miRNAs predicted to target *Fmr1* are encoded by *Fx-mir* cluster. One of these two miRNAs, *miR-743b-3p*, has the second highest prediction score (Appendix Table S1). We next extended our *in silico* analysis to screen all miRNAs predicted to target *Fmr1* and found that 15 miRNAs in the *Fx-mir* cluster are predicted to target *Fmr1*. Table EV1 provides a list of "high-confidence" miRNAs that had a mirSVR score of < −0.5 (indicated in blue); a number of these were also predicted by the TargetScan algorithm (Table EV1). Some of these high-confidence miRNAs target more than one site, bringing the total number of predicted *Fx-mir*-binding sites in the *Fmr1* 3′UTR to 21.

To address whether the *Fx-mir* cluster has more of a propensity to target *Fmr1* than other testes-expressed genes, we compared the number of predicted *Fx-mir*-binding sites in the 3′UTR of *Fmr1* to the 3′UTR from other genes expressed in testes (Table EV2). This analysis revealed that the *Fmr1* 3′UTR had more predicted target sites than did the 3′UTRs of other randomly chosen genes (Table EV2), four of which (*Ar, Vegf, Dazl,* and *Foxi1*) we empirically showed through reporter analysis are targeted by at least one *Fx-mir* family member. To more systematically address this question, we took advantage of a recent study identifying genes exhibiting enriched expression in Sertoli cells (SCs) [36], the primary testicular cell type that expresses several *Fx-mir* family members (see below). These ~500 SC-enriched genes were identified by RiboTag analysis of testes specifically expressing a tagged ribosomal subunit in SCs [36]. We asked which of these ~500 SC-enriched genes are targeted by *Fx-mir* family members by mining target site predictions (microRNA.org), using a mirSVR score of < −0.5. This analysis revealed that *Fmr1* had more predicted *Fx-mir* target sites than any of the other SC-enriched genes (Fig 2A [red line] and Appendix Table S2), and supports the hypothesis that the *Fx-mir*
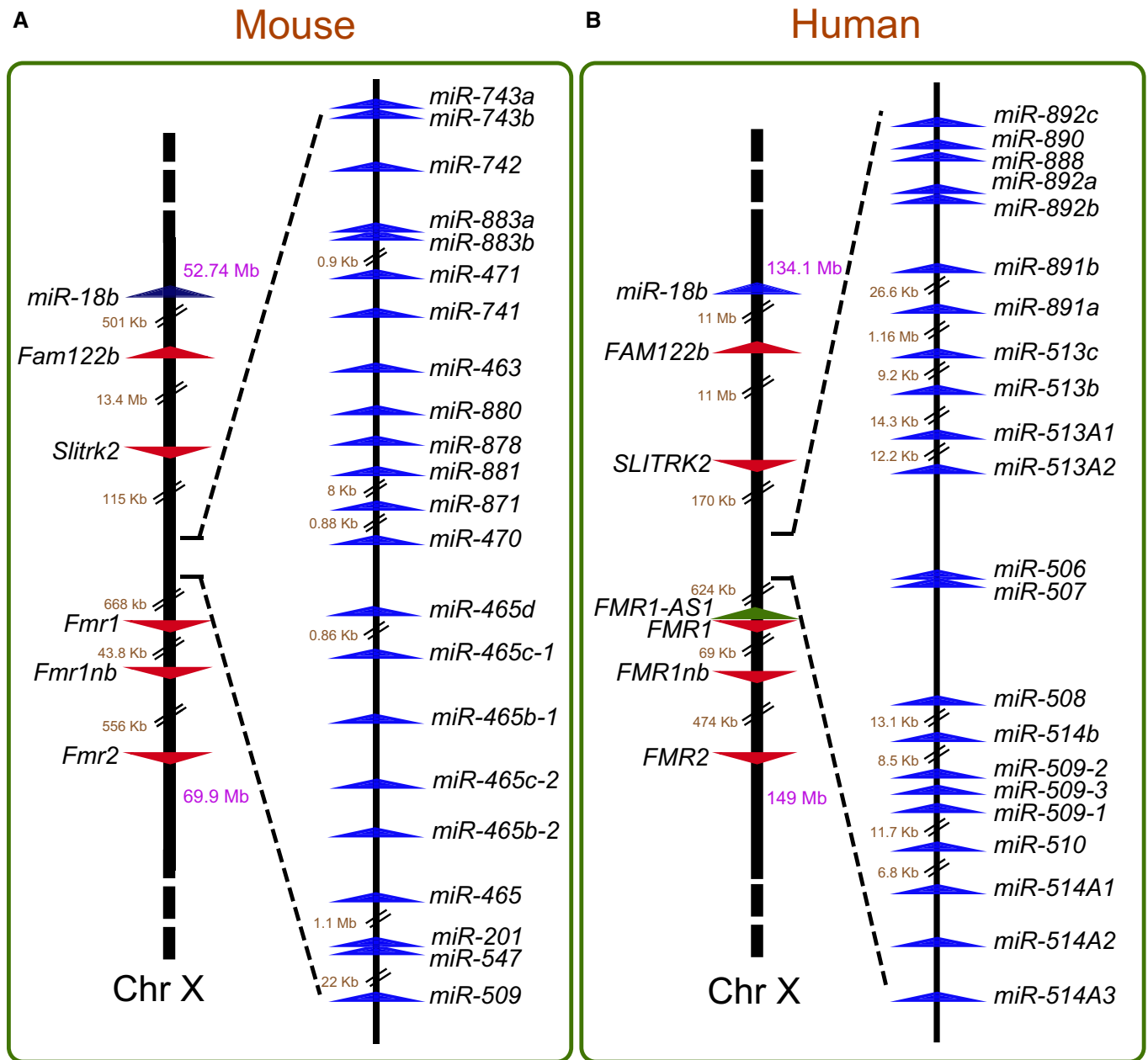
Figure 1.   The mouse and human *Fx-mir* (*FX-MIR*) cluster.

A, B   For each panel, left shows the location of *Fx-mir* cluster (A) or *FX-MIR* cluster (B) on the X chromosome relative to neighboring genes. The numbers in purple represent the chromosomal position of the genes while the numbers in brown indicate intergenic distances. Right shows the relative position of *Fx-mir/FX-MIR* family members, drawn to scale, except when indicated. The arrowheads indicate the transcriptional direction of the genes.

cluster has a strong predilection for targeting the neighboring gene, *Fmr1*.

To empirically test whether *Fx-mir* family members target *Fmr1*, we first employed reporter analysis. The full-length 3′UTR of *Fmr1* was cloned into a firefly luciferase reporter vector, and this reporter was co-transfected into the P19 mouse teratocarcinoma cell line [37] with selected *Fx-mir* miRNA precursors. This analysis identified 6 *Fx-mir* family members that downregulated *Fmr1* 3′UTR-driven reporter expression (Fig 2B; of note, miRNAs without a 5p/3p

designation are from the 5p strand). The reduction in reporter expression was consistent with the known action of most miRNAs, which suppress their targets [38,39]. Downregulation of FMRP by *Fx-mir* family members was also confirmed at the protein level by Western blot analysis (Figs 2C and EV2A).

Given that several *Fx-mir* family members are primarily expressed in SCs (see below), we examined the effect of selected *Fx-mir* miRNAs in MSC1, an established Sertoli cell line that has been used extensively in previous studies to analyze gene regulation in
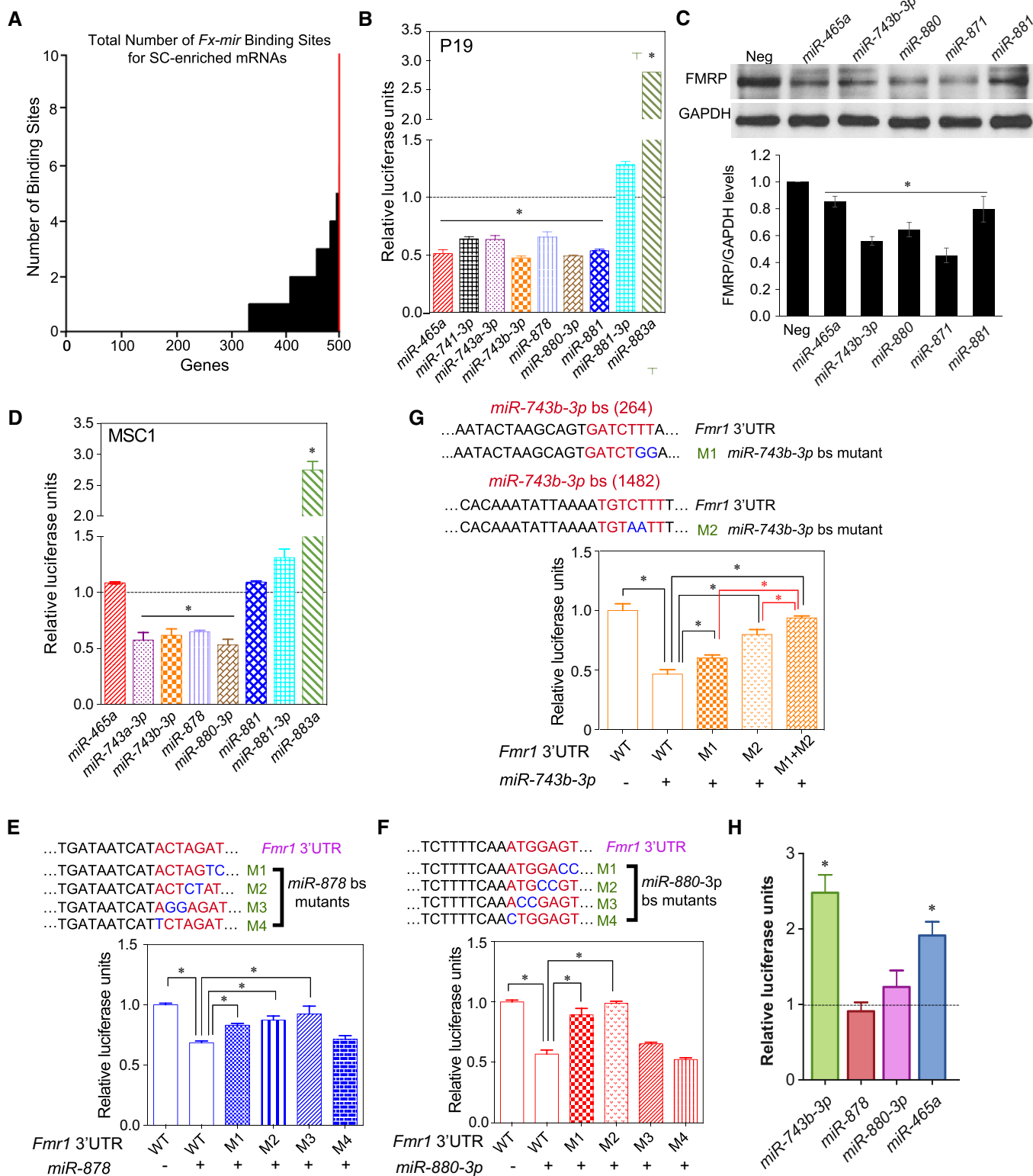
Figure 2.

SCs [27,40,41]. MSC1 cells do not express *Fx-mir* family members (Fig EV2B), consistent with the fact that several SC-enriched genes are turned off when SCs are established in culture [42,43]. However, the MSC1 cell line maintains many characteristics of SCs [42,44],

and its low/undetectable expression of *Fx-mir* miRNAs allowed us to take a gain-of-function approach to analyze the function of *Fx-mir* miRNAs in SCs. Transfection analysis in MSC1 cells revealed that several of the miRNAs we tested downregulated *Fmr1* 3'UTR-driven

Figure 2. Mouse *Fx-mir* family members directly regulate *Fmr1*.

A   Number of *Fx-mir* predicted binding sites in mouse SC-enriched genes. The *Y*-axis shows the number of binding sites predicted from microRNA.org target site predictions, and the *X*-axis shows the number of genes targeted with 0–10 sites. The red line is *Fmr1*.

B–D   Luciferase analysis of P19 cells (panel B) and MSC1 cells (panel D) co-transfected with the pMIR-luciferase reporter harboring the mouse *Fmr1* 3′UTR and the indicated *Fx-mir* miRNA precursors. A Renilla luciferase vector was co-transfected to normalize for transfection efficiency. The luciferase activity of cells transfected with a negative-control scrambled precursor is set to 1. (C) Western blot analysis of endogenous FMRP protein levels in P19 cells transfected with respective *Fx-mir* miRNAs or a negative-control miRNA precursor. The bottom panel shows mean FMRP levels relative to the internal control (GAPDH).

E–G   Luciferase analysis of MSC1 cells co-transfected with (i) a miRNA precursor or a negative-control scrambled miRNA precursor and (ii) the pMIR-luciferase reporter with the wild-type version of the mouse *Fmr1* 3′UTR or mutant versions with the indicated predicted miRNA-binding site (bs) mutations. The seed sequences are depicted in red and the mutations are in blue. *miR-878* (panel E) and *miR-880* (panel F) have one major predicted binding sites, while *miR-743b-3p* (panel G) has three predicted binding sites, two of which were mutated, as described in the text. A Renilla luciferase vector was co-transfected to normalize for transfection efficiency.

H   Luciferase analysis of GS cells co-transfected with the pMIR-luciferase reporter harboring the mouse *Fmr1* 3′UTR and the indicated *Fx-mir* miRNA competitors. The luciferase activity of cells transfected with a negative-control scrambled competitor is set to 1.

Data information: In (B–H), the bars in the histogram represent three independent biological replicates. Data are presented as mean ± SEM. *$P < 0.05$ (Student's *t*-test). Source data are available online for this figure.

reporter expression (Fig 2D). However, two of the miRNAs that repressed *Fmr1* reporter expression in P19 cells—*miR-881* and *miR-465a* (Fig 2B)—did not have a significant effect when force expressed in MSC1 cells (Fig 2D). This is not because MSC1 cells express endogenous *miR-881* and *miR-465a*; indeed, neither MSC1 nor P19 cells express detectable levels of these miRNAs (Fig EV2C and D). Transfection of *miR-881* and *miR-465a* precursors generated levels of these miRNAs in MSC1 cells similar to that of a *Fx-mir* family member (*miR-878*) that does downregulate the *Fmr1* reporter (Figs 2D and EV2D), indicating that the lack of effect of *miR-881* and *miR-465a* on the reporter in MSC1 cells is not due to low expression. The explanation we favor is that cell type-specific factors are responsible for the differential activity of these miRNAs in P19 and MSC1 cells. As precedence for this, a recent study identified tissue-specific miRNA-silencing complexes [45].

Figure EV3A shows the high-confidence binding sites for *Fx-mir* family members predicted to target the *Fmr1* 3′UTR. While these predicted binding sites lie throughout the length of the *Fmr1* 3′UTR, they tend to be clustered in three regions. The specific sequences of some of these predicted binding sites and their complementarity with specific *Fx-mir* miRNAs are shown in Fig EV3B. To test their functionality, we mutated the candidate miRNA-binding sites for three miRNAs in the *Fx-mir* cluster that downregulated *Fmr1* 3′UTR-mediated reporter expression in both MSC1 and P19 cells (Figs 2B and D). All eight nucleotides complementary with the miRNA seed region and beyond were mutated (two in a given mutant construct) to fully analyze the contribution of the seed complementarity region. Figure 2E and F show the data for *miR-878* and *miR-880-3p*, both of which have only one strong predicted binding site in *Fmr1* 3′UTR. Gain-of-function studies with their respective miRNA precursors showed that 3 of the 4 *miR-878* mutants had a statistically significant reduction in miRNA-mediated repression of reporter activity. The M3 and M2 mutants exhibited an almost complete loss of repression in response to the *miR-878* and *miR-880-3p* precursors, respectively. Together, this provided strong evidence that *miR-878* and *miR-880-3p* directly target *Fmr1*. *miR-743b-3p* has three predicted binding sites in the *Fmr1* 3′UTR (Fig EV3A); we made several mutations in the two predicted binding sites with stronger prediction scores [named "264 nt" and "1,482 nt", based on their position within the 3′UTR (Table EV1)]. None of these mutants strongly reduced responsiveness to *miR-743b-3p* (Fig EV3C), raising the possibility that these two sites act redundantly. To test this, we

generated a 264/1,482 double mutant and found it almost completely lost its ability to respond to *miR-743b-3p* (Fig 2G). This indicated that *miR-743b-3p* acts through two partially redundant binding sites in the *Fmr1* 3′UTR to repress *Fmr1* expression.

We next took a loss-of-function approach to validate that *Fx-mir* family members regulate *Fmr1*. We screened for cell lines that express *Fx-mir* family members and found that most cell lines lacked detectable expression (data not shown). The one exception was germline stem (GS) cells (Fig EV3D), a spermatogonial stem cell line that retains stem cell potential [46]. Using miRNA competitors, we repressed *Fx-mir* family members we found were expressed in GS cells. Reporter analysis revealed that repression of *miR-465a* and *miR-743b-3p* elevated the expression of the *Fmr1*-driven reporter (Fig 2H), confirming our gain-of-function evidence that these miRNAs target *Fmr1* (Figs 2B–D). In contrast, *Fmr1*-driven reporter expression was not significantly affected by repression of *miR-878* and *miR-880-3p*, perhaps because these miRNAs can act redundantly as suggested by our miRNA mixing experiments shown below. We did not perform further experiments with GS cells as they exhibit inefficient transfection efficiency (data not shown) [47].

Mouse *Fx-mir* miRNAs exhibit developmentally regulated expression in SCs

In what biological context does the *Fx-mir* cluster function to regulate *Fmr1*? It has been previously shown that many of the miRNAs in the *Fx-mir* cluster exhibit a testis-preferential or testis-specific expression pattern [48–50]. To examine their expression pattern in more detail, we chose to focus on four *Fx-mir* family members targeting *Fmr1*. Three of these miRNAs (*miR-743b-3p, miR-878,* and *miR-880-3p*) have the highest prediction scores for targeting *Fmr1* of all *Fx-mir* family members (Table EV1) and the fourth miRNA (*miR-741-3p*) exhibited strong down-regulation of an *Fmr1* 3′UTR reporter (Fig 2B), despite having a low prediction score (Table EV1). We found that all four of these miRNAs are most highly expressed in the testis (Fig 3A), confirming previous reports [51,52]. These miRNAs were also expressed in the epididymis (the organ where sperm mature and are stored), but at ~10-fold lower level than in the testis (Fig 3A). We also tested members of the rat *Fx-mir* cluster and found they also exhibited testes-enriched expression (Fig EV4A).
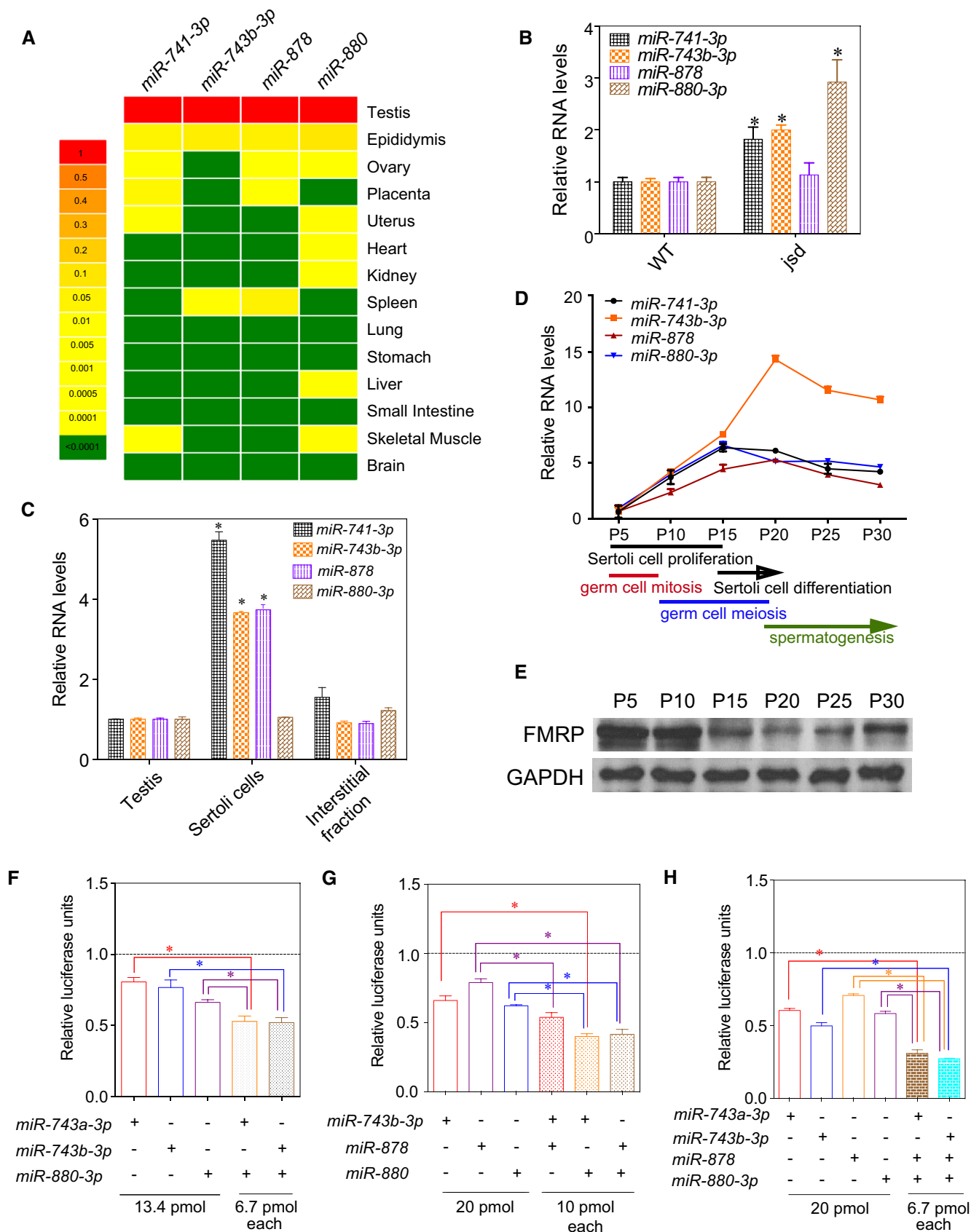
Figure 3.

Figure 3. Developmentally regulated expression and additive action of mouse *Fx-mir* family members.

A   The steady-state levels of *Fx-mir* miRNAs in the indicated adult mouse tissues, as assessed by TaqMan-qPCR analysis. U6 levels were used to normalize miRNA values.

B   TaqMan-qPCR analysis of testes from three *jsd* mice and three control littermate mice. U6 snRNA levels were used for normalization.

C   *Fx-mir miRNA* levels in total mouse testis and different testicular cell fractions assessed by TaqMan-qPCR analysis. U6 snRNA levels were used for normalization.

D   TaqMan-qPCR analysis of testes from the indicated postnatal time points (*n* = 3 for each time point). U6 levels were used to normalize miRNA values.

E   Western blot analysis of mice testes from the indicated postnatal time points.

F–H   Luciferase analysis of MSC1 cells co-transfected with the pMIR-luciferase reporter harboring the mouse *Fmr1* 3′UTR and the indicated *Fx-mir* miRNAs (*n* = 3). The luciferase activity of cells transfected with a negative-control scrambled precursor is set to 1. A Renilla luciferase vector was co-transfected to normalize for transfection efficiency.

Data information: In (B–D and F–H), the bars in the histogram represent three independent biological replicates. Data are presented as mean ± SEM. *$P < 0.05$ (Student's *t*-test).

Source data are available online for this figure.

The testes-enriched expression of members of the *Fx-mir* cluster raises the possibility it regulates *Fmr1* in this organ. Consistent with this possibility, FXS patients lacking *FMR1* expression have macro-orchidism and defects in spermatogenesis [53,54]. These defects are recapitulated in *Fmr1*-null mice [55]. While the underlying cellular mechanism for the generation of large testes is not known, a likely possibility is SC over-expansion, based on finding that *Fmr1*-null mice have hyper-proliferative SCs [56]. Also consistent with this possibility is the finding that the protein product of *Fmr1*—FMRP—is highly expressed in SCs in both mice and humans [57,58]. Thus, in order for *Fx-mir* family members to regulate *Fmr1* in a physiological context, it is critical that these miRNAs are also expressed in SCs. To assess this, we used two approaches. First, we assayed their expression in germ cell-deficient mice. If they are primarily expressed in SCs, their testicular expression should be increased in these mice, as somatic cells are enriched in germ cell-deficient testes. Indeed, 3 of 4 of the *Fx-mir* miRNAs we tested exhibited elevated expression in germ cell-deficient testes relative to control testes (Figs 3B and EV4B). Second, we purified enriched SCs and found that they expressed high levels of *Fx-mir* miRNAs (Figs 3C and EV4C). Three of the 4 miRNAs are expressed at higher levels in purified SCs than total testis, indicating that SCs are the primary site of their expression. We note that it has been previously reported that *Fx-mir* miRNAs are expressed in germ cell-enriched fractions [48,52,59], a finding we reproduced, but we found that expression in the germ cell fractions was much lower than in the total testis fraction (Fig EV4D). Whether this low signal represents trace *Fx-mir* expression in germ cells or contamination of the germ cell fraction with *Fx-mir*-expressing SCs remains to be determined.

SCs are nurse cells in contact with all stages of germ cells and are critical for virtually all phases of spermatogenesis [60,61]. SCs undergo a series of programmed events during the first wave of spermatogenesis; thus, we next examined the expression of *Fx-mir* miRNAs during this developmental time window (Fig 3D). We found that all 4 mRNAs we tested are expressed at low level at P5, when both SCs and germ cells are undergoing rapid proliferation. Their expression dramatically elevates at later time points (Fig 3D), coincident with a drop in FMRP protein expression (Fig 3E). *miR-741-3p* and *miR-880-3p* reach their highest expression at P15, a time point that coincides with the cessation of SC proliferation and the initiation of SC terminal maturation [62,63]. Thus, these two miRNAs are candidates to regulate the expression of mRNAs important for this proliferation-to-maturation transition phase of SC development. This possibility is particularly enticing given that SCs are

known to undergo hyperproliferation in *Fmr1*-null mice [56]. *miR-743b-3p* and *miR-878* exhibited peak expression slightly later, at P20, when SCs undergo further maturation and germ cells initiate differentiation by forming round spermatids. Given that germ cells are in direct contact with SCs [64], this supports a model in which *miR-743b-3p* and *miR-878* regulate gene expression in SCs to influence germ cell differentiation. In support of the possibility that the *Fx-mir* cluster is important for spermatogenesis, a recent study reported that several human *FX-MIR* family members—including *miR-891b, miR-892b, miR-892a, miR-888*, and *miR-890*—are dysregulated in men with asthenozoospermia [65].

Mouse *Fx-mir* miRNAs act additively to repress *Fmr1* expression

miRNAs typically downregulate their mRNA targets by only ~20–40% [66]. To amplify their regulatory effect, several miRNAs must work in conjunction to strongly downregulate a given target mRNA. Our finding that several *Fx-mir* family members that target *Fmr1* 3′UTR (Fig EV3A) are co-expressed in SCs during the same developmental window (Figs 3C and D) raised the possibility that they work together to strongly regulate *Fmr1*. To test this hypothesis, we examined whether combinations of *Fx-mir* family members have greater effects than do single-family members. In support, we found that several *Fx-mir* miRNAs had additive effects (Figs 3F and G). Of note, an additive effect was observed even though we treated the cells with only a half-dose (6.7 pmol) of each miRNA when provided in combination, as compared to the full dose (13.4 pmol) when provided singly (Fig 3F). Given that *miR-878, miR-743b-3p,* and *miR-880* all exhibited additive effects in various combinations (Fig 3G), we also tested a combination of all three of these miRNAs and found that this elicited a very strong repression (~80%) that was much more pronounced than elicited by the individual miRNAs (Fig 3H).

Mouse *Fx-mir* miRNAs regulate the FMRP-eIF4E-CYFIP1 translational regulatory complex

Having demonstrated that *Fx-mir* family members downregulate *Fmr1* expression, we next asked whether *Fx-mir* family members can affect *Fmr1* function. Given that the protein product of *Fmr1*, FMRP, is a translation repressor, we examined whether *Fx-mir* miRNAs affect this function. We chose to examine the FMRP-regulated gene, interferon regulatory factor 1 (*Irf1*), as it encodes a protein involved in spermatogenesis: It promotes germ cell survival *in vitro* and

Figure 4.

◀
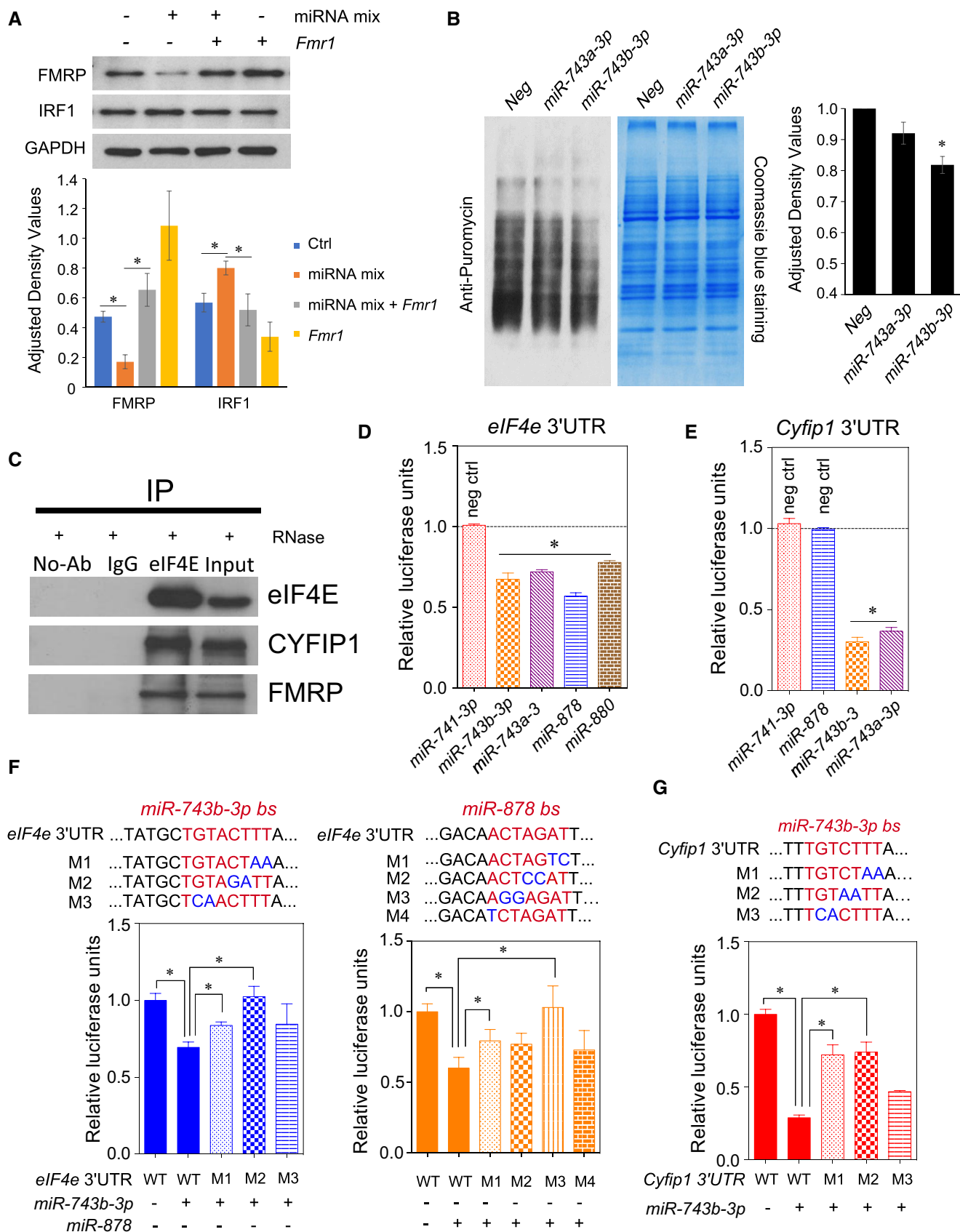
Figure 4. ***Fx-mir* miRNAs target translation regulatory factors.**

A   *Fx-mir* miRNAs repress FMRP function. Top, Western blot analysis of P19 cells transfected with a pool of *Fx-mir* miRNAs targeting *Fmr1* (*miR-743b-3p*, *miR-878*, and *miR-880-3p*) and/or a *Fmr1* expression vector. Bottom, quantification of the Western blot.

B   *miR-743b-3p* reduces protein synthesis. Left, P19 cells were transfected with negative-control miRNAs or the indicated *Fx-mir* miRNAs 42 h prior to the addition of puromycin in the culture medium. The blot was probed with an antibody to puromycin (which detects newly synthesized proteins) and subsequently stained with Coomassie Blue to control for loading. Right, quantification of puromycin incorporation.

C   FMRP, eIF4E, and CYFIP1 interact in the testis. Immunoprecipitation of testis lysates with eIF4E or IgG control antibody, followed by Western blot analysis with the indicated antibodies. The testis lysate was incubated with RNase A to exclude RNA-dependent protein–protein interactions. The input sample is the whole testes lysate (5% relative to volume used for immunoprecipitation).

D, E   *Fx-mir* miRNAs target the translation factors eIF4E and CYFIP1. Luciferase analysis of MSC1 cells co-transfected with the pMIR-luciferase reporter harboring the indicated full-length 3′UTR and the indicated *Fx-mir* miRNAs. *miR-741-3p* was used to demonstrate specificity for regulation of *Eif4e*, as this miRNA does not have a predicted binding site in *Eif4e* 3′UTR. Likewise, *miR-741-3p* and *miR-878* were used to demonstrate specificity for *Cyfip1*, as these miRNAs do not have binding sites in the *Cyfip1* 3′UTR. The luciferase activity of cells transfected with a negative-control scrambled precursor is set to 1. A Renilla luciferase vector was co-transfected to normalize for transfection efficiency.

F, G   Mutagenesis analysis demonstrates that *Eif4e* and *Cyfip1* mRNA are *Fx-mir* direct targets. Luciferase analysis of MSC1 cells co-transfected with (i) a miRNA precursor or a negative-control scrambled miRNA precursor and (ii) the pMIR-luciferase reporter harboring the wild-type version of the mouse *Eif4e and Cyfip1* 3′UTR or mutant versions with the indicated predicted miRNA-binding site (bs) mutations. The seed sequences are depicted in red and the mutations are in blue. A Renilla luciferase vector was co-transfected to normalize for transfection efficiency.

Data information: In (A, B, and D–G), the bars in the histogram represent three independent biological replicates. Data are presented as mean ± SEM. *$P < 0.05$ (Student's *t*-test).

Source data are available online for this figure.

in vivo, and functions as a pro-mitogenic factor in spermatogonia [67]. Transfection analysis showed that forced expression of a pool of three *Fx-mir* miRNAs downregulated FMRP protein level and increased IRF1 protein level (Fig 4A). *Irf1* mRNA level was not significantly altered by this treatment (Fig EV5A), consistent with FMRP acting as a translational repressor [67]. The upregulation of IRF1 was reversed by FMRP overexpression (Fig 4A). Taken together, these data suggest that *Fx-mir* family members regulate FMRP levels, which, in turn, allow them to regulate FMRP function.

Given that FMRP translationally regulates hundreds of mRNAs [32–34], we hypothesized that *Fx-mir* family members influence translation globally. To test this hypothesis, we used SUnSET, a nonradioactive puromycin end-labeling assay that quantifies global protein synthesis [68]. Using this approach, we found that forced expression of *miR-743b-3p* significantly decreased protein synthesis (Fig 4B). Two lines of evidence argue against this being the result of cellular toxicity. First, P19 viable cell count and morphology were not significantly affected by forced *miR-743b-3p* expression (data not shown). Second, transfection of neither a related miRNA (*miR-743a-3p*), nor a scramble-sequence negative-control miRNA, significantly affected global translation (Fig 4B). As an independent approach to assess the effect of *miR-743b-3p* on translation, we used Click-iT metabolic labeling, which labels newly synthesized proteins with the methionine analog, L-azidohomoalanine (AHA). This analysis verified that *miR-743b-3p* significantly represses translation (Fig EV5B). While the effect of *miR-743b-3p* on global translation rate was relatively modest (~20%), it has the potential to be physiologically relevant, as the translation rate of large batteries of mRNAs would presumably be affected. If, instead, *miR-743b-3p* exerted strong translational silencing, this would be expected to instead cause toxicity, as does strong translational silencing during viral infections [69].

In neurons, FMRP regulates translation through forming a translational regulatory complex with two other proteins: eIF4E and CYFIP1 [70]. eIF4E is a rate-limiting translation initiation factor essential for translation, while CYFIP1 is an eIF4E-binding protein that represses translation [70,71]. To test whether this complex exists in the testis,

we performed co-immunoprecipitation experiments. In support, we found both FMRP and CYFIP1 were immunoprecipitated from testes extracts by an eIF4E antibody but not control IgG or no antibody (Fig 4C). We conclude that FMRP, eIF4E, and CYFIP1 interact together in the testes just as they do in neurons.

In silico analysis showed that the 3′UTR regions of *Eif4e* and *Cyfip1* are predicted to be targeted by several *Fx-mir* family members (Table EV3), and thus, we next tested whether *Fx-mir* miRNAs regulate eIF4E and CYFIP1. After cloning their full-length 3′UTRs into the pMIR-luciferase vector, we performed transfection analysis in MSC1 Sertoli cells and found that luciferase activity from the reporter harboring either the *Eif4e* 3′UTR or *Cyfip1* 3′UTR was repressed by several *Fx-mir* family members (Fig 4D and E). As negative controls, we tested miRNAs not predicted to target these two 3′UTRs and found that, indeed, they had no significant effects (Fig 4D and E). Analogous experiments performed in P19 cells revealed similar effects as in MSC1 cells (Fig EV5C and D), suggesting that these miRNAs have a broad ability to regulate *Eif4e* and *Cyfip1*. Mutagenesis of the *miR-743b-3p* and *miR-878* predicted binding sites in the mouse *Eif4e* 3′UTR relieved miRNA-mediated repression (Fig 4F). Many mutants exerted statistically significant effects, while others exerted a trend toward relieved repression. The same was observed for the *miR-743b-3p* predicted binding site in the *Cyfip1* 3′UTR (Fig 4G). We conclude that some *Fx-mir* family members directly target not only *Fmr1*, but also *Eif4e* and *Cyfip1*. This finding, coupled with the expression pattern of these miRNAs in SCs, supports a model in which specific *Fx-mir* family members modulate the translation rate of batteries of mRNAs that are critical to shift SCs from a proliferative to differentiated cell state.

The human *FX-MIR* cluster largely shares the expression pattern of the mouse *Fx-mir* cluster

We next turned our attention to the human *FX-MIR* cluster. To assess its expression characteristics, we examined the levels of 20 mature miRNAs derived from this cluster in human tissues. We found that all 20 of these human *FX-MIR* miRNAs are highly

expressed in the testis (Fig 5A), just as we showed was the case for mouse and rat *Fx-mir* miRNAs (Figs 3A and EV4A). However, the human *FX-MIR* cluster differs from the mouse *Fx-mir* cluster in being expressed in other adult tissues (Fig 5A). miRNAs expressed from the 5′ region of the *FX-MIR* cluster tend to be expressed in ovary, while miRNAs expressed from the 3′ region tend to be expressed in brain and heart. Both 5′ and 3′ miRNAs are expressed in kidney. Together, this indicates that while high testis expression is a conserved feature of the *Fx-mir* cluster, the human version of this cluster has diversified its expression, including the brain, where *FMR1* is highly expressed [57].

Given that mouse *Fx-mir* miRNAs are expressed in SCs (Fig 3B and C), we assessed whether this might also be the case for human *FX-MIR* miRNAs. Toward this end, we obtained RNA from Sertoli cell-only (SCO) patients, who largely or completely lack germ cells in their seminiferous tubules. If human *FX-MIR* family members are expressed in SCs, their expression relative to total testis RNA would be expected to be higher in SCO testes than in normal testes. Consistent with this, we found that 6 of the 7 *FX-MIR* family members we tested exhibited elevated (~2- to 6-fold) expression in SCO testes as compared to normal testes (Fig 5B). As a positive control, we tested the expression of SC markers (*FSHR, AMH, SOX9*) and found they were also upregulated in SCO testes (Fig EV5E). These data strongly suggest that *FX-MIR* miRNAs are most prominently expressed in SCs and/or other somatic cells in the human testis.

Given that some human *FX-MIR* family members are modestly expressed in brain (Fig 5A), this raised the possibility that the *FX-MIR* cluster has a role in FXS. Because the *FX-MIR* cluster is directly adjacent to *FMR1*, the latter of which is methylated and transcriptionally inactivated in neurons in FXS [72], this raised the possibility that the inactive chromatin at the *FMR1* locus has spread to the *FX-MIR* cluster and thereby repressed the expression of its miRNAs in FXS. To test this hypothesis, we used NanoString Technology to assay the expression of the *FX-MIR* miRNAs in neuronal progenitor cells (NPCs) and differentiated neurons derived from iPSC lines generated from FXS patients and control individuals. This analysis showed that several *FX-MIR* miRNAs had significantly dysregulated expression in FXS NPCs and neurons (Fig 5C and D, and Appendix Table S3). However, the expression of the *FX-MIR* cluster was not broadly repressed, strongly suggesting that the inactive chromatin from the *FMR1* locus had not spread to the *FX-MIR* cluster. Indeed, two *FX-MIR* miRNAs (*miR-509-3p* and *miR-890*) had significantly elevated expression in FXS NPCs relative to control NPCs. A similar trend of regulation was seen in neurons where *FX-MIR* family members were both downregulated and upregulated. As observed in NPCs, neurons upregulated *miR-509-3p* and *miR-890* (by ~78-fold and ~106-fold, respectively). The finding that a subset of *FX-MIR* miRNAs are dysregulated in FXS raises the interesting possibility that these particular miRNAs have a role in FXS.

The human *FX-MIR* cluster targets *FMR1*

As described above, the sequences of the miRNAs in the human *FX-MIR* cluster and mouse *Fx-mir* cluster are extremely divergent, such that only one clear miRNA ortholog can be discerned (Appendix Fig S1B). This presented an opportunity to ask a unique question—has the *FX-MIR* cluster retained the ability to target translation regulatory factors despite the rapid divergence in the sequence of the

miRNAs it encodes? As a first step to assess whether members of the human *FX-MIR* cluster target *FMR1*, we screened the 2,588 candidate human miRNAs available in miRBase for their ability to target *FMR1* using the miRNA target prediction programs, micro-RNA.org and TargetScan. This revealed that 2 of the 15 human miRNAs exhibiting the highest prediction scores for targeting *FMR1* are encoded by the human *FX-MIR* cluster (Appendix Table S1). In total, *FMR1* is predicted to be targeted by 13 human *FX-MIR* miRNAs (microRNA.org), six of which are high-confidence targets with strong prediction scores (both microRNA.org and TargetScan), and multiple predicted binding sites (Fig 5E, Table EV4). The total number of predicted *FX-MIR* miRNA-binding sites in the *FMR1* 3′UTR is 26.

To experimentally test the validity of this computational analysis, we cloned the full-length human *FMR1* 3′UTR into a luciferase reporter vector and tested the activity of three human *FX-MIR* family members. We found that two of them—*miR-513a-3p* and *miR-891b*—elicited statistically significant repression in luciferase expression from the reporter vector harboring the human *FMR1* 3′UTR (Fig 5F). The third miRNA, *miR-888*, triggered a trend toward reduced expression but was not statistically significant. Together with our computational analysis, the data indicate that the *FX-MIR* cluster has retained its ability to regulate *FMR1* despite its rapid evolution.

As detailed above, we obtained several lines of evidence that the Fragile-X gene—*Fmr1*—is a strongly favored target of miRNAs encoded by the mouse *Fx-mir* cluster. To assess whether the same is the case for the human *FX-MIR* cluster, we first examined three genes (*SOX9, FSHR*, and *GJA1*) known to be highly expressed in human SCs [73–75], the main cell type that expresses several *FX-MIR* family members (Fig 5B). As shown in Table EV5, the mRNA encoded by these three SC-expressed genes all had fewer predicted binding sites for the 24 known *FX-MIR* family members than did *FMR1* (Table EV5). We also examined the top 20 genes enriched for expression in human neonatal SCs, as defined by single-cell RNAseq analysis (Song *et al,* manuscript in preparation), and found that most of the mRNAs from these genes had far fewer predicted *FX-MIR* family member-binding sites than did *FMR1* mRNA (Table EV5). The only exception—*CALD1*—had 12 predicted *FX-MIR*-binding sites, the same number as for *FMR1*. Together, these data support the notion that, like the mouse *Fx-mir* cluster, the human *FX-MIR* cluster has a predilection for targeting *FMR1*.

Discussion

In this study, we report that the Fragile-X gene, *FMR1*, is targeted for repression by a large cohort of miRNAs expressed from a miRNA cluster adjacent to it. This property appears to be conserved, as we found that the *Fx-mir* cluster is directly adjacent to *Fmr1* across all placental mammals we examined. This predilection for targeting *Fmr1* was unexpected given that miRNAs function *in trans* and thus have the potential to target virtually any gene in the genome.

Why is *Fmr1* a frequent target of a miRNA cluster adjacent to it? One possibility is that close proximity allows for common regulatory elements to drive the coordinated expression of *Fmr1* and the *Fx-mir* cluster, which, in turn, would allow for more efficient regulation. Consistent with this possibility, *Fmr1* and *Fx-mir* family members have similar expression patterns. *Fmr1* is highly expressed in mouse
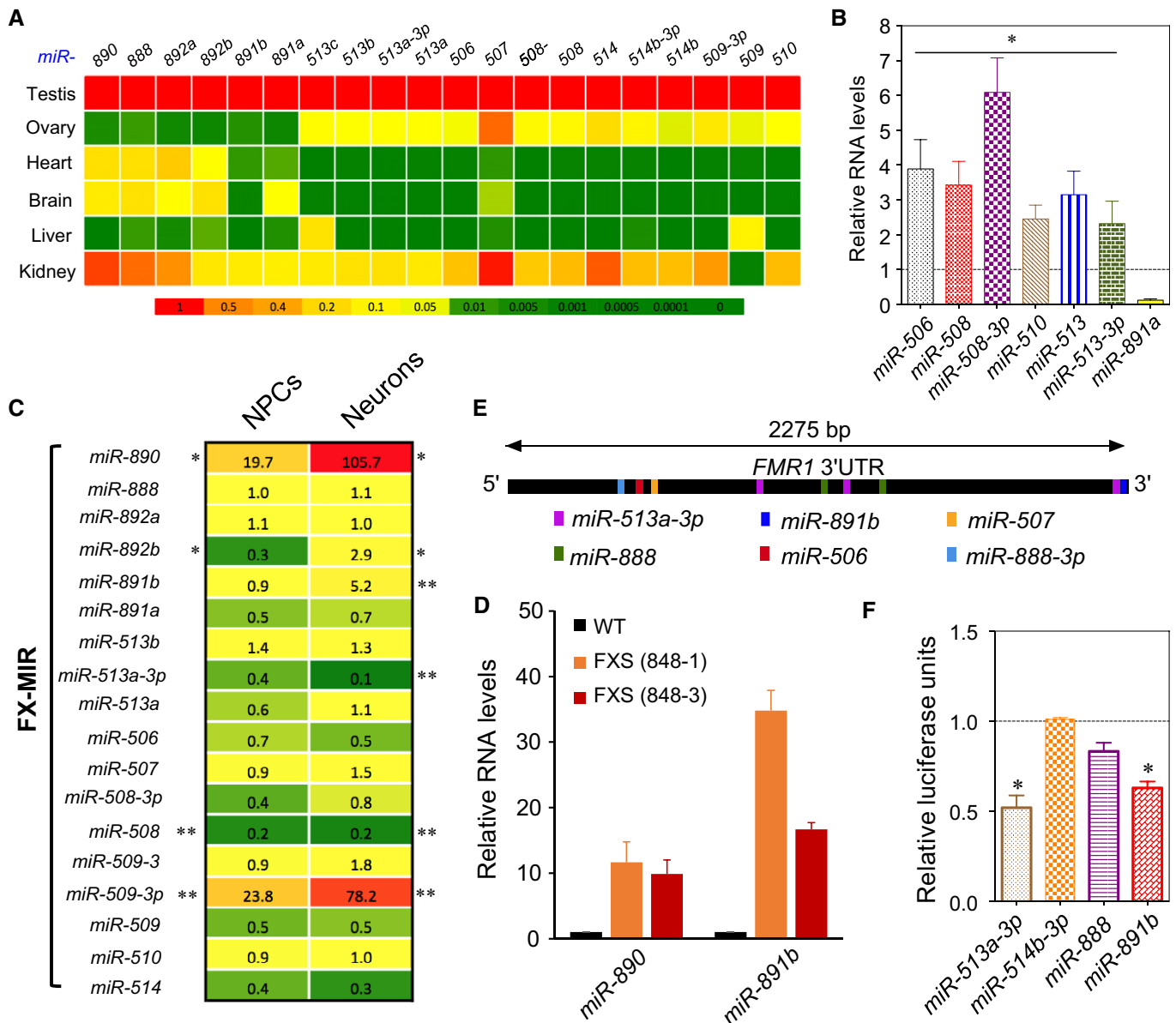
Figure 5. Expression and function of human *FX-MIR* miRNAs.

A Heat map depicting the steady-state levels of *FX-MIR* miRNAs in the indicated adult human tissues, as assessed by TaqMan-qPCR analysis. U6 snRNA levels were used for normalization.

B *FX-MIR* miRNAs are enriched in human Sertoli cell-only (SCO) patient samples. Average values from TaqMan-qPCR analysis of testes biopsies from three SCO patients and three controls. The control values are set as 1. U6 snRNA levels were used for normalization.

C Heat map depicting the relative expression (fold difference) of *FX-MIR* family members in FXS patient versus healthy control iPSC-derived NPC lines and neurons. *0.05 < P < 0.1; **P < 0.05.

D Expression of selected human *FX-MIR* miRNAs in FXS cells. TaqMan-qPCR analysis of human *miR-890* and *miR-891b* in neurons differentiated from iPSC lines generated from FXS patients and control individuals. The expression level in control cells is set at a value of 1. U6 snRNA levels were used for normalization.

E Location of human *FX-MIR*-binding sites along the length of the human *FMR1* 3′UTR.

F Evidence that human *FX-MIR* miRNAs repress human *FMR1* expression. Luciferase analysis of HeLa cells co-transfected with the pMIR-luciferase reporter harboring the human full-length *FMR1* 3′UTR and the indicated *FX-MIR* miRNAs (n = 3). The luciferase activity of cells transfected with a negative-control scrambled precursor is set to 1. A Renilla luciferase vector was co-transfected to normalize for transfection efficiency.

Data information: In (B and F), the bars in the histogram represent three independent biological replicates. Data are presented as mean ± SEM. *P < 0.05 (Student's *t*-test).

testis, which is also the primary site of *Fx-mir* expression [48,76,77]. Likewise, in humans, both FMRP and *FX-MIR* miRNAs are expressed in the brain and the testis [78]. Also, consistent with the possibility of common regulatory elements driving their expression, *Fmr1* and the *Fx-mir* miRNA cluster have a head-to-head configuration. Strikingly, all the miRNAs in both the human *FX-MIR* and mouse *Fx-mir*

clusters exhibit the same transcriptional orientation, which is consistent with the possibility that many or all of them are derived from a long primary transcript driven by a single promoter. This architecture allows for a dedicated regulatory domain housing enhancer elements that can act on both *Fmr1* and the *Fx-mir* cluster. As precedent for the notion of common regulatory elements driving non-coding and coding RNAs, Hu *et al* [79] identified bidirectional promoters driving the transcription of mRNAs and lncRNAs in opposite directions in neurons. While co-expression of the *Fx-mir* cluster and *Fmr1* allows the former to regulate the latter in the same cell types, we suggest that the *Fx-mir* cluster is also likely to be independently regulated from *Fmr1*. Layering independent regulation on top of coordinate regulation would allow members of the *Fx-mir* cluster to modulate *Fmr1* expression in response to specific stimuli.

A non-mutually exclusive explanation for the propensity of the *Fx-mir* cluster to target *Fmr1* is the *Fx-mir* cluster originated from an ancient *Fmr1* gene. In support of this possibility, the primordial *Fmr1* gene is known to have spawned duplicate copies of itself. Several autosomal paralogs of *Fmr1* currently exist in vertebrate genomes [80]. We suggest that in addition to dispersing paralogs to other chromosomes, a primordial *Fmr1* gene also generated a duplicated copy directly adjacent to itself. Duplicated copies of genes often are generated in tandem arrays through the process of "unequal crossing over", a type of gene duplication event that occurs at only low frequency during mitosis and meiosis, but once it occurs, it can be selected for over evolutionary time. If *Fmr1* was duplicated in this manner, one copy may have degenerated into an expressed pseudogene that lost its ability to generate a protein and acquired an ability to generate miRNAs. In favor of this "miRNA birth" hypothesis, miRNAs have been shown to form relatively easily during short periods of evolutionary time [18]. An attractive model is the *Fx-mir* cluster was derived from a duplicated copy of the *Fmr1* gene transcribed in the antisense direction, as such miRNAs would automatically exhibit a predilection for targeting *Fmr1* because they would be complementary to *Fmr1* mRNA. Regardless of the mechanism(s) responsible for *Fmr1* and *Fx-mir* occupying the same genomic neighborhood, once this genomic arrangement was established, it may have been maintained by a mechanism that prevents genomic rearrangements. Such a rearrangement-suppression mechanism has been postulated to be responsible for *Hox*-regulatory miRNAs being retained in *Hox* gene clusters in multiple species [81]. Indeed, there is evidence that miRNAs tend to exhibit conserved gene order relative to protein-coding genes [82]. This conservation may serve to maintain an optimal genomic environment for the expression and function of miRNAs.

Why does the *Fx-mir* cluster harbor such a large number of miRNAs? One possibility is this cluster expanded as a result of selection to exert strong regulation on *Fmr1* and other key target mRNAs. Single miRNAs typically only downregulate their mRNA targets by ~20–40%, and thus, multiple miRNAs are typically required to confer stronger regulation [66]. Indeed, we found that combinations of two *Fx-mir* family members more strongly repressed *Fmr1* 3′UTR-driven reporter expression than did single-family members; a combination of 3 *Fx-mir* family members conferred particularly strong (~80%) downregulation. Previous studies have shown that more pronounced regulation is conferred when miRNA-binding sites are in close proximity (< 40 nt) [82,83]. Thus, it is of interest that we observed additive effects of multiple *Fx-mir* family members even

though their binding sites are relatively far apart in the *Fmr1* 3′UTR (between 94 and 625 nt apart; see the Results section). The ability of combinations of *Fx-mir* miRNAs to strongly regulate *Fmr1* expression raises the possibility that these miRNAs may not only serve as "fine tuners", but also serve as biological switches. In particular, *Fmr1* may be a key target that serves in such circuitry, as we found that *Fmr1* 3′UTR-mediated reporter expression was repressed by very low doses (0.6 pmol) of some *Fx-mir* family members (*miR-878* and *miR-880-3p*; data not shown).

A conserved feature of the *Fx-mir* cluster is its high expression in the testis. Intriguingly, we obtained evidence that the primary cell type expressing the *Fx-mir* cluster in both humans and mice is the SC, which is a large somatic cell in direct contact with all stages of developing male germ cells. SCs provide factors and an appropriate niche that support all steps of spermatogenesis. We found that two mouse *Fx-mir* family members, *miR-741-3p* and *miR-880-3p*, are most highly expressed when rodent SCs cease proliferation and undergo terminal maturation. Thus, these miRNAs are candidates to regulate the expression of key target mRNAs important for this proliferation-to-maturation transition phase of Sertoli cell development. Two other miRNAs in the mouse *Fx-mir* cluster, *miR-878* and *miR-743b-3p*, display highest expression at a slightly later point of development—P20—when SCs undergo further maturation and the most advanced germ cells are undergoing the transition from meiosis to differentiation [79,80]. Other members of the *Fx-mir* cluster, including *miR-743a-3p and miR-883a*, have been shown to display peak expression during this same ~P15 to ~P20 time window [48], raising the possibility that many miRNAs from the *Fx-mir* cluster cooperate to drive or fine-tune events that occur during this critical somatic and germ cell developmental time period.

While rodents primarily express the *Fx-mir* cluster in the testis, we found that humans express *FX-MIR* cluster in other tissues, including the brain. It has been often noted that many genes are co-expressed in the testes and the brain, but the evolutionary forces driving this expression pattern and the functional consequences of it are not known [84,85]. The expression of the *FX-MIR* cluster in both brain and testis in humans is of interest given that its major target, *FMR1*, is particularly highly expressed in these two particular organs, as described above [78,86]. Thus, the *FX-MIR* cluster may regulate translation in cells in both of these two organs through its ability to repress FMRP levels.

The rapid sequence divergence of the X-linked *Fx-mir* cluster is consistent with a wide body of work showing that X-linked and testes-expressed genes tend to undergo rapid evolution [76–80]. Increasing evidence suggests that the testis is birthplace of many genes and has a permissive environment for gene expression and therefore has a particularly diverse transcriptome [40,76]. This is not restricted to protein-coding genes, as studies have shown that miRNAs in their rapidly evolving phase also commonly exhibit restricted expression in the testis [81–83]. Indeed, the *Fx-mir* cluster appears to be fairly young, which may contribute to its rapid evolution.

The rapid evolution of the *Fx-mir* cluster presents an interesting dilemma. While *Fx-mir* sequence alterations permit the miRNAs expressed from this cluster to regulate new target mRNAs, how do they retain the ability to regulate previous critical mRNA targets? We suggest that in some cases, miRNAs and their critical targets undergo co-evolution, such that sequence alterations in the miRNAs

select for corresponding sequence alterations in the mRNA target to maintain sequence complementarity. In the case of coordinately regulated miRNA clusters such as the *Fx-mir* cluster, a flexible approach may be used to achieve this goal, such as a "division of labor" approach in which "old" and "new" mRNA targets are regulated by different family members. In support, we found that many seemingly unrelated miRNAs in the human and mouse *Fx-mir* clusters targeted *Fmr1*, raising the possibility that selective forces acting on independent miRNAs were responsible for maintaining *Fmr1* regulation in the primate and rodent lineages. Thus, in spite of the rapid divergence of sequence, both the mouse and human *Fx-mir* clusters are able to efficiently target *Fmr1*. Thus, the *Fx-mir* cluster may be a useful model to study miRNA clusters at an intermediate point of evolution that are rapidly acquiring new mRNA targets ("new friends") but also maintaining a subset of their old mRNA targets ("old friends").

Functional conservation in the face of rapid sequence evolution is a growing theme in biology. For example, Ulitsky *et al* identified lincRNAs that have conserved roles in embryonic development in zebrafish and humans despite the fact they exhibit little sequence conservation between these two species [84]. These lincRNAs maintain their location in the genomes of diverse species, just as we showed is the case for the rapidly evolving *Fx-mir* cluster. Another example of maintenance of function in the face of sequence diversity is transcription factor *cis*-regulatory elements, which have been shown to maintain the ability to regulate specific genes and transcriptional programs despite undergoing rapid changes in sequence [85]. Indeed, retention of precise transcription factor binding sites appears to be the exception, rather than the rule, over evolutionary time. For example, the *Endo16* promoter, while divergent in sequence in two sea urchin species, *Strongylocentrotus purpuratus* and *Lytechinus variegatus,* maintains its transcription pattern during larval development in these two species [86]. Similarly, the enhancer elements in the *even skipped* locus in *Drosophila* and scavenger flies are highly divergent in sequence, yet they drive identical expression patterns in transgenic *Drosophila* embryos [87].

In conclusion, we have defined a new miRNA cluster and found that a large cohort of miRNAs expressed from this cluster target *Fmr1*, the gene directly adjacent to it in all placental mammals we examined. Several members of the *Fx-mir* cluster target not only *Fmr1*, but also mRNAs encoding other proteins that form a regulatory complex with FMRP. This result, coupled with our finding that many members of the *FX-MIR* cluster are expressed in human neurons and SCs, raises the possibility that one function of this miRNA cluster is to control the translation of batteries of mRNAs in these seemingly unrelated somatic cells. In the future, it will be important to determine the clinical consequences of dysregulated *FX-MIR* expression.

Materials and Methods

Mammalian cell culture, transfections, and luciferase assays

MSC1 and HeLa cells were grown in DMEM (Invitrogen), 10% fetal calf serum, and 1× penicillin/streptomycin. P19 cells were grown in MEMα (Invitrogen), 10% fetal calf serum, and 1× penicillin/

streptomycin (Invitrogen). All cells were cultured at 37°C with 5% CO_2. For transfection experiments, the cells were trypsinized and seeded in 24-well plates at a density of ~50,000 cells per well. The cells were transiently transfected using Lipofectamine 2000 (Invitrogen), following the manufacturer's instructions. The transfections were carried out with 20 pmol of miRNA precursor, 20 ng of firefly luciferase vector, and 10 ng of the Renilla luciferase vector. Dual luciferase analysis (using a Renilla Luciferase vector for normalization) was performed according to the manufacturer's instructions (Promega, Cat. no. E1960) on lysates prepared 24 h post-transfection. Statistical significance was determined using the paired Student's *t*-test.

Testis cell fractionation

Sertoli and interstitial cells were purified from testes as previously described [41]. In brief, testes were decapsulated and the seminiferous tubules were allowed to settle in PBS, followed by incubation in collagenase (C2674; Sigma). After another round of settling, the pellet and supernatant were used as the source of SCs and interstitial (mainly Leydig) cells, respectively. To obtain enriched SCs, the pellet was resuspended in a solution containing 0.1% collagenase, 0.2% hyaluronidase (H6254; Sigma), 0.04% DNase I (D5025; Sigma), and 0.03% trypsin inhibitor (T6522; Sigma) in 1× PBS (pH 7.4) at 30°C for 40 min. The SCs were purged of contaminating germ cell by hypotonic shock (incubation in 1:7 diluted PBS for 3 min). To obtain enriched Leydig cells, the supernatant obtained after collagenase treatment was pelleted and subjected to the same hypotonic shock treatment as the SCs.

3′UTR cloning

The full-length 3′UTR of *Fmr1*, *Eif4e*, and *Cyfip1* were PCR-amplified from mouse and/or human testis cDNA, and then cloned into pMIR-REPORT vector, which lacks a 3′UTR (Ambion, Cat. no. AM5795).

Site-directed mutagenesis

Site-specific mutagenesis was performed, as previously described [87], to generate the mutant versions of the 3′UTR reporter vectors. The primers used to generate the mutants are provided in Appendix Table S4.

miRNA quantification

Total cellular RNA was isolated from cells and tissues using TRIzol (Invitrogen). TaqMan-qPCR was performed (in triplicate for each sample) using TaqMan® microRNA assays (Applied Biosystems).

Real-time PCR analysis

Total cellular RNA was isolated using TRIzol (Invitrogen), as previously described [27]. Reverse transcription–PCR analysis was performed by first generating cDNA from 1 μg of total cellular RNA using iSCRIPT (Bio-Rad), followed by PCR amplification using SYBR Green and the ΔΔCt method (with ribosomal L19 for normalization).

Protein analysis

For Western blot analysis, cells were harvested in radioimmunoprecipitation assay (RIPA) buffer supplemented with protease inhibitor cocktail (Sigma, Cat. no. P8340) and phenylmethylsulfonylfluoride (PMSF). Following incubation in lysis buffer on ice for 30 min, the samples were centrifuged at 16,050 g for 15 min at 4°C, and the lysates were transferred to new tubes, and protein level was quantified using the DC™ Protein Assay kit (Bio-Rad, Cat. no. 500-0112). Twenty micrograms of the protein samples was separated on an 8–12% polyacrylamide gel, and Western blot analysis was performed as previously described [41].

For anti-puromycin detection of newly synthesized proteins, the image from gel electrophoresis was captured and the membrane was stained with Coomassie Blue to verify equal loading in all lanes. Densitometric measurements were performed by determining the density of each whole lane (incorporating the entire molecular weight range of puromycin-labeled proteins) using ImageJ software (U.S. National Institutes of Health, Bethesda, MD, USA; https://imagej.nih.gov/ij/). Details of the antibodies used are provided in Appendix Table S5.

Protein synthesis was also measured using the L-azidohomoalanine (AHA) Click-iT (Thermo Fisher Scientific, C10102) metabolic labeling reagents, following the manufacturer's protocol. Briefly, cultured P19 cells were washed twice with warmed PBS and incubated in methionine-free DMEM (Thermo Fisher Scientific, 21013024) for 1 h. The medium was replaced with methionine-free DMEM to which 50 μM of the methionine analog AHA was added. After incubation, the dishes were rinsed twice. Newly synthesized proteins labeled with Click-iT AHA were conjugated with the tetramethylrhodamine alkyne (TAMRA) using the Click-iT™ Tetramethylrhodamine (TAMRA) Protein Analysis Detection Kit (Thermo Fisher Scientific, C33370). Protein samples were separated on 10% SDS–PAGE and visualized using 532 nm excitation. The gel was subsequently stained with Coomassie blue for normalization.

Immunoprecipitation analysis

Testis from 1-month-old BL6 mice were harvested, decapsulated, and immediately put into 400 μl of ice-cold lysis buffer (10 mM Tris–HCl pH 7.5, 10 mM NaCl, 2 mM EDTA) supplemented with PMSF, protease inhibitor cocktail, and phosphatase inhibitor cocktail (Phosphatase Arrest I, G-Biosciences, Cat. no. 786-450). The decapsulated testes were crushed with a pestle and incubated, with intermittent inversion, in the lysis buffer for 15 min on ice. NaCl was then added to all the samples at a final concentration of 150 mM, and the indicated samples were treated with 5 μl of RNase A (10 mg/ml). The tubes were inverted and subjected to gentle vortex before 10 min of incubation on ice. The lysates were then spun at maximum speed for 15 min at 4°C, and the supernatant was used for IP analysis. Protein G sepharose beads (Invitrogen, Inc.) were prepared for IP analysis by washing them twice with NET-2 buffer (50 mM Tris–HCl pH 7.5, 150 mM NaCl, 0.05% Triton-X 100). 40 μl of a 100 mg/ml bead slurry was incubated with 5 μl of either eIF4E polyclonal antibody or purified rabbit IgG (5 μg) resuspended in NET-2 buffer supplemented with PMSF, protease inhibitor, and phosphatase arrest and incubated overnight at 4°C. The antibody-coupled beads were washed three times with NET-2 buffer with gentle centrifugation inbetween (250 g for 1 min). The washed antibody-coupled beads were left on ice until the testis lysates were ready to be incubated. Testes lysates (400 μl), prepared as described above, were incubated for 2–4 h on ice. The beads were then washed eight times with NET-2 buffer with gentle centrifugation inbetween. After the last wash, most of the supernatant was removed, 10 μl of SDS–polyacrylamide gel electrophoresis (PAGE) loading buffer was added, the beads were vortexed, boiled for 5 min, vortexed again, centrifuged at maximum speed (13,000 g), and the supernatant was loaded on a 12% polyacrylamide gel for Western blot analysis.

Control and Fragile-X Syndrome neural progenitor and differentiated neuron preparation

Fibroblasts from a clinically healthy male control (GM08330) or a diagnosed Fragile-X Syndrome male patient (GM05848) were purchased from Coriell Institute for Medical Research and used to derive induced pluripotent stem cell (iPSC) clones and subsequent stable, homogeneous neural progenitor cells (NPCs) as described [88]. NPCs were expanded in 70% DMEM (Invitrogen), 30% Ham's F-12 (Mediatech), supplemented with B-27 (Invitrogen), 20 ng/ml EGF (Sigma), and 20 ng/ml bFGF (R&D Systems) on poly-ornithine (Sigma)/laminin (Sigma)-coated culture plates. Neural differentiation was induced by growth factor removal in the same media for 15 days before harvest. Cells were harvested by scraping and pelleting followed by total RNA (including miRNAs) isolation using a miRNeasy Mini Kit (Qiagen). Biological triplicates were collected from each undifferentiated NPC and differentiated neuron cultures from control 8330-8 and two clones from the FXS patient: 848-1 and 848-3 [88].

NanoString nCounter miRNA profile analysis

miRNAs were processed with the NanoString nCounter system (NanoString, Seattle, Washington, USA) per vendor instructions with chipsets of Human miRNA v.1 (664 endogenous miRNAs and five housekeeping transcripts). Data archiving, normalization, analysis, and file export were performed using nSolver software v.2.5 (NanoString). Probe intensity data between samples were normalized using nSolver Software utilizing either the geometric means of five housekeeping genes (ACTB, B2M, GAPDH, RPL19, and RPLP0) or geometric mean normalization of the highest 100 values within each sample. For the purpose of comparison, control samples ($n = 3$ from each condition) were compared to combined FXS samples from both 848-1 and 848-3 (thus $n = 6$ from each condition).

Expanded View for this article is available online.

Author contributions

MR and MFW conceived the project. MR, KT, T-DMP, and MW designed experiments. MR, KT, T-DMP, H-WS, JND, SJ, and EYS performed experiments. SDS and SJH performed the NanoString nCounter miRNA Profile work. MR, KT, T-DMP, H-WS, JND, SJ, EYS, KJP, JG, HC-A, and MFW analyzed the data. MR, KT, T-DMP, and MFW wrote the paper.

Conflict of interest

The authors declare that they have no conflict of interest.

References

1. Kutter C, Watt S, Stefflova K, Wilson MD, Goncalves A, Ponting CP, Odom DT, Marques AC (2012) Rapid turnover of long noncoding RNAs and the evolution of gene expression. *PLoS Genet* 8: e1002841

2. Nasvall J, Sun L, Roth JR, Andersson DI (2012) Real-time evolution of new genes by innovation, amplification, and divergence. *Science* 338: 384–387

3. Swanson WJ, Vacquier VD (2002) The rapid evolution of reproductive proteins. *Nat Rev Genet* 3: 137–144

4. Ellegren H, Parsch J (2007) The evolution of sex-biased genes and sex-biased gene expression. *Nat Rev Genet* 8: 689–698

5. Meiklejohn CD, Parsch J, Ranz JM, Hartl DL (2003) Rapid evolution of male-biased gene expression in *Drosophila*. *Proc Natl Acad Sci USA* 100: 9894–9899

6. Torgerson DG, Singh RS (2004) Rapid evolution through gene duplication and subfunctionalization of the testes-specific alpha4 proteasome subunits in *Drosophila*. *Genetics* 168: 1421–1432

7. Haerty W, Jagadeeshan S, Kulathinal RJ, Wong A, Ravi Ram K, Sirot LK, Levesque L, Artieri CG, Wolfner MF, Civetta A *et al* (2007) Evolution in the fast lane: rapidly evolving sex-related genes in *Drosophila*. *Genetics* 177: 1321–1335

8. Turner LM, Chuong EB, Hoekstra HE (2008) Comparative analysis of testis protein evolution in rodents. *Genetics* 179: 2075–2089

9. Brawand D, Soumillon M, Necsulea A, Julien P, Csardi G, Harrigan P, Weier M, Liechti A, Aximu-Petri A, Kircher M *et al* (2011) The evolution of gene expression levels in mammalian organs. *Nature* 478: 343–348

10. Wang X, Zhang J (2004) Rapid evolution of mammalian X-linked testis-expressed homeobox genes. *Genetics* 167: 879–888

11. Stevenson BJ, Iseli C, Panji S, Zahn-Zabal M, Hide W, Old LJ, Simpson AJ, Jongeneel CV (2007) Rapid evolution of cancer/testis genes on the X chromosome. *BMC Genom* 8: 129

12. Singh ND, Petrov DA (2007) Evolution of gene function on the X chromosome versus the autosomes. *Genome Dyn* 3: 101–118

13. Llopart A (2012) The rapid evolution of X-linked male-biased gene expression and the large-X effect in *Drosophila* yakuba, *D. santomea*, and their hybrids. *Mol Biol Evol* 29: 3873–3886

14. Meisel RP, Malone JH, Clark AG (2012) Faster-X evolution of gene expression in *Drosophila*. *PLoS Genet* 8: e1003013

15. Fabian MR, Sonenberg N, Filipowicz W (2010) Regulation of mRNA translation and stability by microRNAs. *Annu Rev Biochem* 79: 351–379

16. Djuranovic S, Nahvi A, Green R (2011) A parsimonious model for gene regulation by miRNAs. *Science* 331: 550–553

17. Ha M, Kim VN (2014) Regulation of microRNA biogenesis. *Nat Rev Mol Cell Biol* 15: 509–524

18. Meunier J, Lemoine F, Soumillon M, Liechti A, Weier M, Guschanski K, Hu H, Khaitovich P, Kaessmann H (2013) Birth and expression evolution of mammalian microRNA genes. *Genome Res* 23: 34–45

19. Vidigal JA, Ventura A (2015) The biological functions of miRNAs: lessons from *in vivo* studies. *Trends Cell Biol* 25: 137–147

20. Bracken CP, Scott HS, Goodall GJ (2016) A network-biology perspective of microRNA function and dysfunction in cancer. *Nat Rev Genet* 17: 719–732

21. Greenberg DS, Soreq H (2014) MicroRNA therapeutics in neurological disease. *Curr Pharm Des* 20: 6022–6027

22. Khazaie Y, Nasr Esfahani MH (2014) MicroRNA and male infertility: a potential for diagnosis. *Int J Fertil Steril* 8: 113–118

23. Tanzer A, Stadler PF (2004) Molecular evolution of a microRNA cluster. *J Mol Biol* 339: 327–335

24. Reddy KB (2015) MicroRNA (miRNA) in cancer. *Cancer Cell Int* 15: 38

25. Iwakawa HO, Tomari Y (2015) The functions of MicroRNAs: mRNA decay and translational repression. *Trends Cell Biol* 25: 651–665

26. Brown V, Jin P, Ceman S, Darnell JC, O'Donnell WT, Tenenbaum SA, Jin X, Feng Y, Wilkinson KD, Keene JD *et al* (2001) Microarray identification of FMRP-associated brain mRNAs and altered mRNA translational profiles in fragile X syndrome. *Cell* 107: 477–487

27. Maclean JA II, Chen MA, Wayne CM, Bruce SR, Rao M, Meistrich ML, Macleod C, Wilkinson MF (2005) Rhox: a new homeobox gene cluster. *Cell* 120: 369–382

28. Bruno IG, Karam R, Huang L, Bhardwaj A, Lou CH, Shum EY, Song HW, Corbett MA, Gifford WD, Gecz J *et al* (2011) Identification of a microRNA that activates gene expression by repressing nonsense-mediated RNA decay. *Mol Cell* 42: 500–510

29. Lou CH, Shao A, Shum EY, Espinoza JL, Huang L, Karam R, Wilkinson MF (2014) Posttranscriptional control of the stem cell and neurogenic programs by the nonsense-mediated RNA decay pathway. *Cell Rep* 6: 748–764

30. Shum EY, Jones SH, Shao A, Dumdie J, Krause MD, Chan WK, Lou CH, Espinoza JL, Song HW, Phan MH *et al* (2016) The antagonistic gene paralogs Upf3a and Upf3b govern nonsense-mediated RNA decay. *Cell* 165: 382–395

31. Huang L, Shum EY, Jones SH, Lou CH, Dumdie J, Kim H, Roberts AJ, Jolly LA, Espinoza JL, Skarbrevik DM *et al* (2017) A Upf3b-mutant mouse model with behavioral and neurogenesis defects. *Mol Psychiatry* 23: 1773–1786

32. Li Z, Zhang Y, Ku L, Wilkinson KD, Warren ST, Feng Y (2001) The fragile X mental retardation protein inhibits translation via interacting with mRNA. *Nucleic Acids Res* 29: 2276–2283

33. Zalfa F, Giorgi M, Primerano B, Moro A, Di Penta A, Reis S, Oostra B, Bagni C (2003) The fragile X syndrome protein FMRP associates with BC1 RNA and regulates the translation of specific mRNAs at synapses. *Cell* 112: 317–327

34. Stefani G, Fraser CE, Darnell JC, Darnell RB (2004) Fragile X mental retardation protein is associated with translating polyribosomes in neuronal cells. *J Neurosci* 24: 7272–7276

35. Betel D, Koppal A, Agius P, Sander C, Leslie C (2010) Comprehensive modeling of microRNA targets predicts functional non-conserved and non-canonical sites. *Genome Biol* 11: R90

36. De Gendt K, Verhoeven G, Amieux PS, Wilkinson MF (2014) Genome-wide identification of AR-regulated genes translated in Sertoli cells *in vivo* using the RiboTag approach. *Mol Endocrinol* 28: 575–591

37. van der Heyden MA, Defize LH (2003) Twenty one years of P19 cells: what an embryonal carcinoma cell line taught us about cardiomyocyte differentiation. *Cardiovasc Res* 58: 292–302

38. Bartel DP (2009) MicroRNAs: target recognition and regulatory functions. *Cell* 136: 215–233

39. Huntzinger E, Izaurralde E (2011) Gene silencing by microRNAs: contributions of translational repression and mRNA decay. *Nat Rev Genet* 12: 99−110

40. McGuinness MP, Linder CC, Morales CR, Heckert LL, Pikus J, Griswold MD (1994) Relationship of a mouse Sertoli cell line (MSC-1) to normal Sertoli cells. *Biol Reprod* 51: 116−124

41. Hu Z, Dandekar D, O'Shaughnessy PJ, De Gendt K, Verhoeven G, Wilkinson MF (2010) Androgen-induced Rhox homeobox genes modulate the expression of AR-regulated genes. *Mol Endocrinol* 24: 60−75

42. Steinberger A, Jakubowiak A (1993) Sertoli cell culture: historical perspective and review of methods. In *The Sertoli cell*, Russell L, Griswold M (eds), pp 155−180. Clearwater, FL: Cache River Press

43. Sutton KA, Maiti S, Tribley WA, Lindsey JS, Meistrich ML, Bucana CD, Sanborn BM, Joseph DR, Griswold MD, Cornwall GA *et al* (1998) Androgen regulation of the Pem homeodomain gene in mice and rat Sertoli and epididymal cells. *J Androl* 19: 21−30

44. Russell LD, Steinberger A (1989) Sertoli cells in culture: views from the perspectives of an in vivoist and an in vitrist. *Biol Reprod* 41: 571−577

45. Dallaire A, Frederick PM, Simard MJ (2018) Somatic and germline MicroRNAs form distinct silencing complexes to regulate their target mRNAs differently. *Dev Cell* 47: 239−247.e4

46. Kanatsu-Shinohara M, Ogonuki N, Inoue K, Miki H, Ogura A, Toyokuni S, Shinohara T (2003) Long-term proliferation in culture and germline transmission of mouse male germline stem cells. *Biol Reprod* 69: 612−616

47. Maezawa S, Hasegawa K, Yukawa M, Sakashita A, Alavattam KG, Andreassen PR, Vidal M, Koseki H, Barski A, Namekawa SH (2017) Polycomb directs timely activation of germline genes in spermatogenesis. *Genes Dev* 31: 1693−1703

48. Song R, Ro S, Michaels JD, Park C, McCarrey JR, Yan W (2009) Many X-linked microRNAs escape meiotic sex chromosome inactivation. *Nat Genet* 41: 488−493

49. Devor EJ, Huang L, Wise A, Peek AS, Samollow PB (2011) An X chromosome microRNA cluster in the marsupial species *Monodelphis domestica*. *J Hered* 102: 577−583

50. Linsen SE, de Wit E, de Bruijn E, Cuppen E (2010) Small RNA expression and strain specificity in the rat. *BMC Genom* 11: 249

51. Buchold GM, Coarfa C, Kim J, Milosavljevic A, Gunaratne PH, Matzuk MM (2010) Analysis of microRNA expression in the prepubertal testis. *PLoS ONE* 5: e15317

52. Ro S, Park C, Sanders KM, McCarrey JR, Yan W (2007) Cloning and expression profiling of testis-expressed microRNAs. *Dev Biol* 311: 592−602

53. Santoro MR, Bray SM, Warren ST (2012) Molecular mechanisms of fragile X syndrome: a twenty-year perspective. *Annu Rev Pathol* 7: 219−245

54. Charalsawadi C, Wirojanan J, Jaruratanasirikul S, Ruangdaraganon N, Geater A, Limprasert P (2017) Common clinical characteristics and rare medical problems of fragile X syndrome in Thai patients and review of the literature. *Int J Pediatr* 2017: 9318346

55. The Dutch-Belgian Fragile X Consorthium, Bakker CE, Verheij C, Willemsen R, van der Helm R, Oerlemans F, Vermey M, Bygrave A, Hoogeveen A, Oostra BA *et al* (1994) Fmr1 knockout mice: a model to study fragile X mental retardation. The Dutch-Belgian Fragile X Consortium. *Cell* 78: 23−33

56. Slegtenhorst-Eegdeman KE, de Rooij DG, Verhoef-Post M, van de Kant HJ, Bakker CE, Oostra BA, Grootegoed JA, Themmen AP (1998) Macroorchidism in FMR1 knockout mice is caused by increased Sertoli cell proliferation during testicular development. *Endocrinology* 139: 156−162

57. Devys D, Lutz Y, Rouyer N, Bellocq JP, Mandel JL (1993) The FMR-1 protein is cytoplasmic, most abundant in neurons and appears normal in carriers of a fragile X premutation. *Nat Genet* 4: 335−340

58. Bakker CE, de Diego OY, Bontekoe C, Raghoe P, Luteijn T, Hoogeveen AT, Oostra BA, Willemsen R (2000) Immunocytochemical and biochemical characterization of FMRP, FXR1P, and FXR2P in the mouse. *Exp Cell Res* 258: 162−170

59. McIver SC, Stanger SJ, Santarelli DM, Roman SD, Nixon B, McLaughlin EA (2012) A unique combination of male germ cell miRNAs coordinates gonocyte differentiation. *PLoS ONE* 7: e35553

60. Griswold MD (1998) The central role of Sertoli cells in spermatogenesis. *Semin Cell Dev Biol* 9: 411−416

61. Walker WH, Cheng J (2005) FSH and testosterone signaling in Sertoli cells. *Reproduction* 130: 15−28

62. Kluin PM, Kramer MF, de Rooij DG (1984) Proliferation of spermatogonia and Sertoli cells in maturing mice. *Anat Embryol* 169: 73−78

63. Walker WH (2003) Nongenomic actions of androgen in Sertoli cells. *Curr Top Dev Biol* 56: 25−53

64. Griswold MD (1995) Interactions between germ cells and Sertoli cells in the testis. *Biol Reprod* 52: 211−216

65. Qing X, Shi J, Dong T, Wu C, Hu L, Li H (2017) Dysregulation of an X-linked primate-specific epididymal microRNA cluster in unexplained asthenozoospermia. *Oncotarget* 8: 56839−56849

66. Grimson A, Farh KK, Johnston WK, Garrett-Engele P, Lim LP, Bartel DP (2007) MicroRNA targeting specificity in mammals: determinants beyond seed pairing. *Mol Cell* 27: 91−105

67. Lian J, Tian H, Liu L, Zhang XS, Li WQ, Deng YM, Yao GD, Yin MM, Sun F (2010) Downregulation of microRNA-383 is associated with male infertility and promotes testicular embryonal carcinoma cell proliferation by targeting IRF1. *Cell Death Dis* 1: e94

68. Schmidt EK, Clavarino G, Ceppi M, Pierre P (2009) SUnSET, a nonradioactive method to monitor protein synthesis. *Nat Methods* 6: 275−277

69. Voinnet O (2005) Induction and suppression of RNA silencing: insights from viral infections. *Nat Rev Genet* 6: 206−220

70. Napoli I, Mercaldo V, Boyl PP, Eleuteri B, Zalfa F, De Rubeis S, Di Marino D, Mohr E, Massimi M, Falconi M *et al* (2008) The fragile X syndrome protein represses activity-dependent translation through CYFIP1, a new 4E-BP. *Cell* 134: 1042−1054

71. Culjkovic B, Topisirovic I, Skrabanek L, Ruiz-Gutierrez M, Borden KL (2006) eIF4E is a central node of an RNA regulon that governs cellular proliferation. *J Cell Biol* 175: 415−426

72. Bagni C, Tassone F, Neri G, Hagerman R (2012) Fragile X syndrome: causes, diagnosis, mechanisms, and therapeutics. *J Clin Invest* 122: 4314−4322

73. Baccetti B, Collodel G, Costantino-Ceccarini E, Eshkol A, Gambera L, Moretti E, Strazza M, Piomboni P (1998) Localization of human follicle-stimulating hormone in the testis. *FASEB J* 12: 1045−1054

74. Chui K, Trivedi A, Cheng CY, Cherbavaz DB, Dazin PF, Huynh AL, Mitchell JB, Rabinovich GA, Noble-Haeusslein LJ, John CM (2011) Characterization and functionality of proliferative human Sertoli cells. *Cell Transplant* 20: 619−635

75. Giese S, Hossain H, Markmann M, Chakraborty T, Tchatalbachev S, Guillou F, Bergmann M, Failing K, Weider K, Brehm R (2012) Sertoli-cell-specific knockout of connexin 43 leads to multiple alterations in testicular gene expression in prepubertal mice. *Dis Model Mech* 5: 895−913

76. Bachner D, Steinbach P, Wohrle D, Just W, Vogel W, Hameister H, Manca A, Poustka A (1993) Enhanced Fmr-1 expression in testis. *Nat Genet* 4: 115−116

77. Panneerdoss S, Chang YF, Buddavarapu KC, Chen HI, Shetty G, Wang H, Chen Y, Kumar TR, Rao MK (2012) Androgen-responsive microRNAs in mouse Sertoli cells. *PLoS ONE* 7: e41146

78. Tamanini F, Willemsen R, van Unen L, Bontekoe C, Galjaard H, Oostra BA, Hoogeveen AT (1997) Differential expression of FMR1, FXR1 and FXR2 proteins in human brain and testis. *Hum Mol Genet* 6: 1315−1322

79. Hu HY, He L, Khaitovich P (2014) Deep sequencing reveals a novel class of bidirectional promoters associated with neuronal genes. *BMC Genom* 15: 457

80. Kirkpatrick LL, McIlwain KA, Nelson DL (2001) Comparative genomic sequence analysis of the FXR gene family: FMR1, FXR1, and FXR2. *Genomics* 78: 169−177

81. Yekta S, Tabin CJ, Bartel DP (2008) MicroRNAs in the Hox network: an apparent link to posterior prevalence. *Nat Rev Genet* 9: 789−796

82. Chen J, Chen W, Li Y (2012) Conservation of gene order in human microRNA-neighboring regions. *Genome* 55: 701−704

83. Warth SC, Hoefig KP, Hiekel A, Schallenberg S, Jovanovic K, Klein L, Kretschmer K, Ansel KM, Heissmeyer V (2015) Induced miR-99a expression represses Mtor cooperatively with miR-150 to promote regulatory T-cell differentiation. *EMBO J* 34: 1195−1213

84. Guo JH, Huang Q, Studholme DJ, Wu CQ, Zhao Z (2005) Transcriptomic analyses support the similarity of gene expression between brain and testis in human as well as mouse. *Cytogenet Genome Res* 111: 107−109

85. Guo J, Zhu P, Wu C, Yu L, Zhao S, Gu X (2003) *In silico* analysis indicates a similar gene expression pattern between human brain and testis. *Cytogenet Genome Res* 103: 58−62

86. Peier AM, McIlwain KL, Kenneson A, Warren ST, Paylor R, Nelson DL (2000) (Over)correction of FMR1 deficiency with YAC transgenics: behavioral and physical features. *Hum Mol Genet* 9: 1145−1159

87. Li S, Wilkinson MF (1997) Site-directed mutagenesis: a two-step method using PCR and DpnI. *Biotechniques* 23: 588−590

88. Lue Y, Rao PN, Sinha Hikim AP, Im M, Salameh WA, Yen PH, Wang C, Swerdloff RS (2001) XXY male mice: an experimental model for Klinefelter syndrome. *Endocrinology* 142: 1461−1470